Perspective Error Correction using Registration for Blockface Volume Reconstruction of Serial Histological Sections of the Human Brain

Björn Eiben[1,2], Christoph Palm[1,3], Uwe Pietrzyk[1,3], Christos Davatzikos[4]
Katrin Amunts[1,2]

[1]Institute for Neuroscience and Medicine (INM-1), Research Center Jülich
[2]Institute for Psychiatry and Psychotherapy, RWTH Aachen
[3]Institute for Physics, University Wuppertal
[4]Department of Radiology, University of Pennsylvania
b.eiben@fz-juelich.de

Abstract. For accurate registration of histological sections blockface images are frequently used as three dimensional reference. However, due to the use of endocentric lenses the images suffer from perspective errors such as scaling and seemingly relative movement of planes which are located in different distances parallel to the imaging sensor. The suggested correction of those errors is based on the estimation of scaling factors derived from image registration of regions characterized by differing distances to the point of view in neighboring sections. The correction allows the generation of a consistent three dimensional blockface volume.

1 Introduction

Human post-mortem brains are sectioned with micro- and cryotomes in order to analyze the microstructure of the brain with microscopical resolution in histological and autoradiographic studies. Distortions due to sectioning and other steps of histological processing, however, are inevitable. To correct for these distortions and to perform a three dimensional (3D) reconstruction of the sections, blockface images which show the tissue block prior to cutting each section (Fig. 1(a)), proved to be an important reference modality [1, 2].

Blockface images relate directly to a 3D reference of brain tissue if the imaging setup remains constant during the whole sectioning process. In practice however, the position of the tissue block with respect to the camera is not completely fixed since the block moves against the microtome knife section to section. Furthermore the tissue plane moves away form the camera as the microtome knife is lowered iteratively.

The registration of a reference grid beneath the tissue block does not lead to full 3D consistency of the tissue as it ignores the usage of an endocentric optic and its resulting perspective errors.

2 Materials and Methods

Frozen brain tissue was sectioned into 20 μm coronal sections with a cryostat microtome (Polycut CM 3500, Leica, Germany). The blockface images were taken by a CCD camera with a resolution of 2048 × 2048 pixels (Macrofire, Optronics, Goleta, USA) with an endocentric lens (APO-Componon 4.5/90, Schneider-Kreuznach, Germany). Image acquisition results in a spatial resolution in the reference-grid plane of 95 μm/pixel. The approximate distance of the lenses primary plane to the reference grid is $d = 1.23$ m.

The knife position of the microtome is altered in z-direction from one section to the next, hence the distance of the tissue to the lenses primary plane changes equally between blockface images resulting in decreasing reproduction scales.

Utilizing homogenous coordinates to describe the imaging chain (Fig. 2, [3]), differing positions of the tissue block can be expressed by a displacement matrix $\boldsymbol{V}_n$ which varies slightly for each section n (Fig. 2(a),v 2(b)). The perspective projection of a point is calculated by a multiplication with $\boldsymbol{P}_\measuredangle$. The final step is the parallel projection to the imaging sensor plane expressed by a multiplication with $\boldsymbol{P}_{\shortparallel}$. Thus the perspectively projected point $\boldsymbol{p}_d$ can be described as

$$\boldsymbol{p}_d = \boldsymbol{P}_{\shortparallel} \cdot \boldsymbol{p}_c = \boldsymbol{P}_{\shortparallel} \cdot \boldsymbol{P}_\measuredangle \cdot \boldsymbol{V}_n \cdot \boldsymbol{p}_a = \begin{pmatrix} (x\cos(\alpha) - y\sin(\alpha) + t_x)\frac{d}{z+d} \\ (x\sin(\alpha) + y\cos(\alpha) + t_y)\frac{d}{z+d} \\ 0 \\ 1 \end{pmatrix} \tag{1}$$

$$\boldsymbol{P}_{\shortparallel} := \begin{pmatrix} 1&0&0&0 \\ 0&1&0&0 \\ 0&0&0&0 \\ 0&0&0&1 \end{pmatrix};\ \boldsymbol{P}_\measuredangle := \begin{pmatrix} 1&0&0&0 \\ 0&1&0&0 \\ 0&0&1&0 \\ 0&0&\frac{1}{d}&1 \end{pmatrix};\ \boldsymbol{V}_n := \begin{pmatrix} \cos\alpha & -\sin\alpha & 0 & t_{x,n} \\ \sin\alpha & \cos\alpha & 0 & t_{y,n} \\ 0 & 0 & 1 & 0 \\ 0 & 0 & 0 & 1 \end{pmatrix};\ \boldsymbol{p}^T := \begin{pmatrix} x^T \\ y^T \\ z^T \\ 1 \end{pmatrix}$$

As a first step the reference grid is segmented from all blockface images utilizing a variance filter followed by the analyzation of the Hough-Transformation (Fig. 1(b)). Hence the image domain Ω^I is split into grid Ω^G and background $\Omega^B = \Omega^I \setminus \Omega^G$. Thereafter the grid of each image $I_n(\boldsymbol{x})$, with $1 \leq n \leq N$,

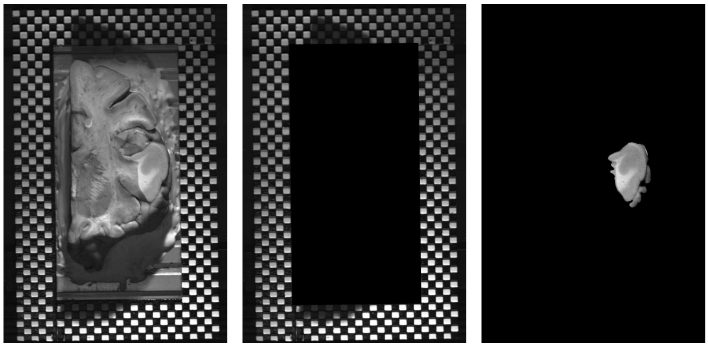

(a) blockface image (b) reference grid (c) tissue

Fig. 1. Blockface images of a frozen tissue block of a human brain.

is rigidly registered to the grid of a central reference image I_c, $c \approx \frac{N}{2}$ by the transformation $\mathcal{T} : \mathbb{Z}^2 \to \mathbb{R}^2$:

$$I_n^{\mathcal{T}_G}(\boldsymbol{x}) := I_n(\mathcal{T}_G(\boldsymbol{x}, \theta)) \quad \text{with} \quad \mathcal{T}_G(\boldsymbol{x}, \theta) := \begin{pmatrix} \cos\alpha & -\sin\alpha \\ \sin\alpha & \cos\alpha \end{pmatrix} \boldsymbol{x} + \begin{pmatrix} t_x \\ t_y \end{pmatrix} \tag{2}$$

The parameters of the rigid transformation θ are rotation by α and translation by $\boldsymbol{t}$. A masked normalized correlation metric m_{NC} guides the rigid registration process to account for illumination changes. It is calculated on those points only where the grid is present in the moving and the fixed image:

$$\Omega_n^{\mathcal{T}_G} := \left\{ \boldsymbol{x} \mid \left(\boldsymbol{x} \in \Omega_c^G \right) \wedge \left(D\left(\mathcal{T}_G(\boldsymbol{x})\right) \in \Omega_n^G \right) \right\} \tag{3}$$

where $D : \mathbb{R}^2 \to \mathbb{Z}^2$ maps to discrete coordinate positions.

$$m_{\mathrm{NC}}\left(I_n^{\mathcal{T}_G}, I_c, \Omega_n^{\mathcal{T}_G}\right) = \frac{\sum_{\boldsymbol{x} \in \Omega_n^{\mathcal{T}_G}} \left(I_n^{\mathcal{T}_G}(\boldsymbol{x}) - \bar{I}_n^{\mathcal{T}_G}\right)\left(I_c(\boldsymbol{x}) - \bar{I}_c\right)}{\sqrt{\sum_{\boldsymbol{x} \in \Omega_n^{\mathcal{T}_G}} \left(I_n^{\mathcal{T}_G}(\boldsymbol{x}) - \bar{I}_n^{\mathcal{T}_G}\right)^2 \sum_{\boldsymbol{x} \in \Omega_n^{\mathcal{T}_G}} \left(I_c(\boldsymbol{x}) - \bar{I}_c\right)^2}} \tag{4}$$

with $\bar{I}_c$ being the mean gray-value of I_c on the overlapping grid domain. The rigid registration parameters are optimized using an evolutionary strategy.

$$\hat{\theta}_n^G = \underset{\theta}{\operatorname{argmax}} \left(m_{\mathrm{NC}}\left(I_n^{\mathcal{T}_G}, I_c, \Omega_n^{\mathcal{T}_G}\right)\right) \tag{5}$$

The obtained registration results describe the block displacement in relation to the central reference image for each section. Different block positions cause different viewpoints from which the tissue block is exposed. This results in a relative movement of tissue and grid in the blockface image since they are positioned in different z-planes (compare y-positions of $\boldsymbol{p}_b^T$ and $\boldsymbol{p}_b^G$ with its perspectively projected points $\boldsymbol{p}_c^T$ and $\boldsymbol{p}_c^G$ in Fig. 2(b)). As a second step registration of the

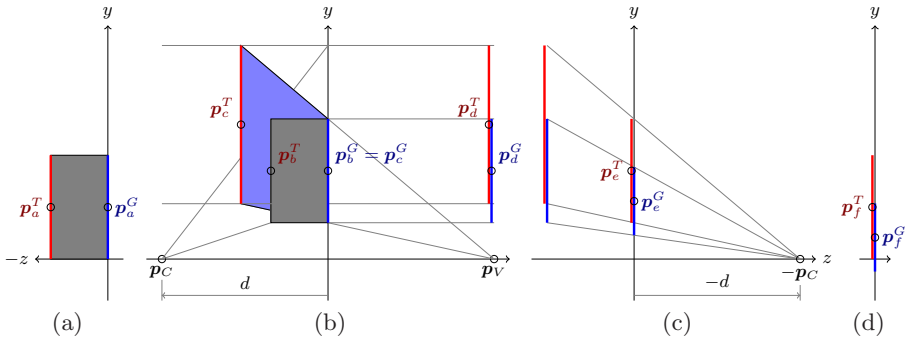

Fig. 2. Perspective distortion and correction. $\boldsymbol{p}^T$ is located on the tissue plane (T) and $\boldsymbol{p}^G$ on the grid (G). The block $\boldsymbol{p_a}$ (a) is displaced $\boldsymbol{p_b}$, perspectively transformed $\boldsymbol{p_c}$ and parallel projected $\boldsymbol{p}_d$ (b). Correct scaling projects the tissue onto the corresponding grid position $\boldsymbol{p_d^G} = \boldsymbol{p_e^T}$ (c). Hence the inverted displacement of the block results in equal y-positions of the corrected point $\boldsymbol{p}_f^T$ (d) and the original point $\boldsymbol{p}_a^T$.

tissue segment (Fig. 1(c)) in neighboring sections compared to the corresponding block positions allows for measuring the relative movement of grid and tissue. The metric of the registration is masked by the tissue segment

$$\Omega_{n+1}^{\mathcal{T}_T} := \left\{ \boldsymbol{x} \mid \left(\boldsymbol{x} \in \Omega_n^I \right) \wedge \left(D(\mathcal{T}_T(\boldsymbol{x})) \in \Omega_{n+1}^T \right) \right\} \tag{6}$$

replacing $\Omega_n^{\mathcal{T}_G}$ in (4) and resulting in the optimized parameters $\hat{\theta}_{n+1}^T$ according to (5). As consecutive sections differ in z-direction by $20\,\mu$m the assumption of no change in z holds true with an acceptable error. Finding the transformations $\boldsymbol{A}_{n+1}^T$ from $\hat{\theta}_{n+1}^T$ and $\boldsymbol{A}_n^G$ from $\hat{\theta}_n^G$ maps the following points to each other:

$$\begin{aligned} \boldsymbol{p}'_{T,n} &= \boldsymbol{A}_n^G \cdot \boldsymbol{P}_{\measuredangle} \left(\boldsymbol{A}_n^G \right)^{-1} \cdot \boldsymbol{p}_T \\ &= \boldsymbol{A}_{n+1}^T \cdot \boldsymbol{P}_{\measuredangle} \left(\boldsymbol{A}_{n+1}^G \right)^{-1} \cdot \boldsymbol{p}_T = \boldsymbol{p}'_{T,n+1} \end{aligned} \tag{7}$$

Comparing the different registrations, which on the one hand align the reference grids and on the other the tissue structures allows to calculate the scaling factor.

$$1 + \frac{z_n}{d} = \frac{t_{y,n}^G - t_{y,n+1}^G}{t_{y,n}^G - t_y^T} \tag{8}$$

Scaling each image by this estimated factor followed by the transformation detected for the reference grid corrects the perspective error (Fig. 2(c) and 2(d)) introduced in (1).

3 Results

A series of 1167 blockface images was used to evaluate the performance of the presented perspective error correction. Block displacements and relative tissue

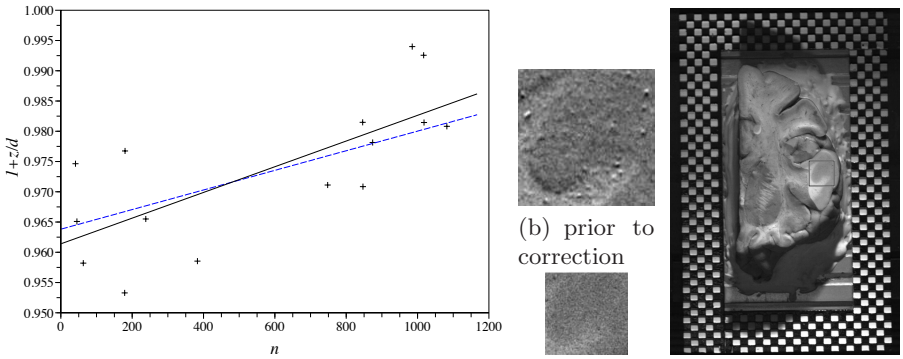

(a) estimated scaling factors

(b) prior to correction

(c) corrected

(d) position

Fig. 3. Results of the depth estimation and correction. Calculations of (8) are marked with +. The linear regression is shown as a solid and the theoretical slope as a dotted line (a). (b) and (c) show the difference of the same consecutive sections without and with perspective error correction for the region marked in (d).

to grid movements were measured by mono-modal rigid image registration which was implemented using the Insight Segmentation and Registration Toolkit. A significant block displacement is necessary to measure the relative movement of tissue and grid. Therefore the evaluation of (8) was limited to sections with block displacements lager than 3 mm. With a correlation coefficient of $\rho = 0.73$ slope and axis in tercept of the scaling factor line are estimated (Fig. 3(a)). Comparing the regression with the samples, a standard deviation of $\sigma = 7.9 \cdot 10^{-3}$ results. Using knowledge about the camera distance d, section number n and the section thickness, a theoretical slope can also be calculated which supports the estimated regression line that was used for correction of the perspective error. Difference images of consecutive sections without and with perspective error correction reveal the enhancement of consistency (Fig. 3 (b-d)).

4 Discussion

The displacement of the grid plane measured by registration is – due to the perspective error – not equal to the displacement of the tissue plane located in a different distance to the point of view. The presented perspective error correction and object scaling estimation is able to calculate and correct for this error. Registration results of neighboring tissue in combination with the measured displacements allow to estimate the tissue scaling. Relative movements of tissue in neighboring sections can be effectively compensated. The perspective error gets more pronounced the thicker the block for sectioning is.

The use of telecentric instead of endocentric lenses avoids perspective errors. The usually required short distance to the object and narrow field of depth however make it not feasible for the use in a cryostat microtome. For the estimation of the scaling factor, visible tissue displacements due to perspective errors need to be distributed over the whole data set in a reasonable number. Otherwise the estimation is likely to become unreliable. The registration results need to be of high accuracy for estimating the scaling factor correctly. If this can be ensured, the presented method allows the perspective error correction without the exact knowledge of the original setting.

Acknowledgement. This study was supported by the IRTG 1328 of the Deutsche Forschungsgemeinschaft (DFG).

References

1. Amunts K, Zilles K. Atlases of the Human Brain: Tools for Functional Neuroimaging. In: Zaborsky L, Wouterlood FG, Lanciego JL, editors. Neuroanatomical Tract-Tracing 3. Springer Berlin/Heidelberg; 2006. p. 566–603.
2. Schormann T, Dabringhaus A, Zilles K. Statistics of deformations in histology and application to improved alignment with MRI. IEEE Trans Med Imaging. 1995;14(1):25–35.
3. Jähne B. Digitale Bildverarbeitung. Springer Berlin/Heidelberg; 2002.